55 1999; Kanda et al. 2000; Timmermann et al. 2001; Inui
56 et al. 2002b; Nakata et al. 2004) showing a similar onset
57 latency between SI and SII activities, while others (Inui
58 et al. 2003a, b) showed an early SI activity prior to the
59 main SII activity, implying serial processing through SI
60 and SII. In addition to MEG, laser-evoked potentials
61 (LEPs) have been used for the temporal assessment of
62 cortical pain processing. Although the SII area was the
63 major cortical region responsible for LEPs in most
64 studies (for review, see Apkarian et al. 2005), several
65 studies reported the involvement of the contralateral
66 SI in pain processing (Tarkka and Treede 1993; Schle-
67 reth et al. 2003; Ohara et al. 2004). Tarkka and Treede
68 (1993) reported that a N1 component at a latency of
69 160 ms was generated in SI and SII, whereas others
70 demonstrated an activity in the contralateral SI helped
71 to shape the N2 component (Schlereth et al. 2003;
72 Ohara et al. 2004). Valeriani et al. (2000) reported an
73 early component with a peak latency of 83 ms originat-
74 ing from SII or the insular area, suggesting that the
75 opercular cortex is also involved in early processing.
76 Therefore, the temporal aspect of the processing of
77 noxious information in the cortex still remains to be
78 elucidated.

79 A laser can activate nociceptors of thinly myelinated
80 A-delta fibers without stimulating tactile afferents, and
81 therefore is a good tool with which to investigate the
82 nociceptive system. However, since the skin's nocicep-
83 tors are activated via temperature conduction by the
84 laser beam, there is considerable jitter in the latency of
85 the activation of nociceptors among trials (Bromm and
86 Treede 1984), which is problematic for studies using an
87 averaging technique. The main activations in SI and
88 SII reported previously (Ploner et al. 1999; Kanda
89 et al. 2000; Timmermann et al. 2001; Nakata et al.
90 2004) are less affected by latency jittering because of
91 their long duration. However, the possibility cannot be
92 excluded that some weak and short-lasting activities at
93 an earlier latency were overlooked due to the problem
94 of jittering in conventional averaging (C-AVE). In the
95 present study, we used latency-corrected averaging to
96 test this possibility.

Methods

97

Subjects

98

99 The experiment was performed on nine healthy male
100 volunteers, aged 27–43 years (32.1 ± 5.3). Informed
101 consent was obtained from all participants prior to the
102 study, which was first approved by the Ethics Commit-
103 tee at our Institute.

Laser stimulation

104

105 A thulium:YAG laser stimulator (Carl Baasel Laser-
106 tech, Starnberg, Germany) was used to elicit noxious
107 stimuli. Laser pulses (1 ms in duration, 2,000 nm in
108 wavelength, and 3 mm in spot diameter) were deliv-
109 ered to the dorsum of the left hand at an interval of
110 between 8 and 12 s. The interstimulus interval of 8–12 s
111 was employed to avoid habituation of evoked cortical
112 responses (Raij et al. 2003). The irradiated points were
113 moved slightly for each stimulus to avoid tissue dam-
114 age and habituation of the receptors. The mean inten-
115 sity was 211 mJ, ranging from 200 to 250 mJ, with
116 which a painful sensation having a visual analysis score
117 (VAS) of around 7 was evoked in each subject. Since
118 the laser stimulator caused large magnetic artifacts, it
119 was set outside the shielded room, and the laser beam
120 was conducted through optical fibers, approximately
121 6.5 m in length, into the shielded room. In order to
122 maintain the distance between the laser outlet and the
123 skin surface, the optical fiber was attached to the MEG
124 device and subjects were instructed to attach the palm
125 of the left hand to the table during the recording.

MEG recording

126

127 Laser-evoked magnetic fields (LEFs) were recorded
128 with a helmet-shaped 306-channel detector array (Vec-
129 torview; ELEKTA Neuromag, Helsinki), which com-
130 prises 102 identical triple sensor elements, in a
131 magnetically shielded room. Each sensor element con-
132 sists of two orthogonal planar gradiometers and one
133 gradiometer magnetically coupled to a multi-supercon-
134 ducting quantum interference device (SQUID) and thus
135 provides three independent measurements of the mag-
136 netic fields, though in this study, results recorded from
137 204 planar gradiometers were analyzed. The signals were
138 recorded with a 0.1–100 Hz bandpass filter and digitized
139 at a sampling rate of 900 Hz. The period of analysis was
140 500 ms including a prestimulus period of 100 ms. Sixty
141 trials following laser stimulation were recorded.

142 Prior to the recording, the exact location of the head
143 with respect to the sensors was found by measuring the
144 magnetic signals produced by currents leading to four
145 indicator coils placed at known sites on the scalp. The
146 four indicator coils attached to the subject's head were
147 measured with respect to the three anatomical land-
148 marks using a 3D digitizer to allow alignment of the
149 MEG and magnetic resonance (MR) image coordinate
150 systems (3.0-T Siemens Allegra). The x-axis was fixed
151 with the preauricular points, the positive direction
152 being to the right. The positive y-axis passed through
153 the nasion and the z-axis thus pointed upward. Current

154 was then fed to the indicator coils and the resulting
155 magnetic fields were measured with the magnetometer,
156 which allowed for aligning the individual head coordi-
157 nate system with the magnetometer coordinate system.

158 Averaging of trials

159 First, C-AVE using the onset of the noxious stimula-
160 tion was done. In C-AVE waveforms, the largest
161 response was usually recorded in the right (hemisphere
162 contralateral to the stimulated side) temporal area
163 (Fig. 1a) at around 150–200 ms after stimulation con-
164 sistent with previous studies (Kakigi et al. 1995; Ploner
165 et al. 1999; Kanda et al. 2000; Timmermann et al. 2001;
166 Nakata et al. 2004). We selected the channel with the
167 largest amplitude around the temporal region as a sen-
168 sor of interest (SOI, Fig. 1a). The peak latency of the
169 SOI was determined in each subject and was used for
170 latency-adjusted averaging (L-AVE).
171 Second, L-AVE was done, in which each trial had
172 been latency-adjusted before the averaging. One prob-
173 lem with a single-trial analysis is that the signal-to-noise
174 ratio (S/N) is very low for single epochs. Notably, high
175 frequency noises superimposed on the evoked response
176 were problematic when determining the peak of the
177 response. After several attempts, we found that a cutoff
178 frequency of 15 Hz is appropriate for determination of
179 the peak latency of the main component. Therefore as a
180 first step, MEG signals of each trial were filtered with a
181 low-pass of 15 Hz. Then we used the SOI to select trials
182 to include averaging (Fig. 1c). That is, only the trials
183 whose SOI had an unambiguous peak within the range
184 of the peak latency of the C-AVE waveform ±20 ms
185 were selected by visual inspection (red traces in Fig. 1c).
186 Such a procedure has been shown to improve S/N ratio
187 of LEP components (Iannetti et al. 2005). Once trials to
188 be included for L-AVE were determined, the original
189 0.1–100 Hz waveforms of the selected trials were then
190 latency-corrected (Fig. 1e), so that the peak of the SOI
191 matched on the time axis and averaged (Fig. 1f).

192 Data analysis

193 First, the source of the main components in C-AVE
194 and L-AVE was estimated in order to know whether
195 the quality of L-AVE was changed as compared with
196 C-AVE. The equivalent current dipole (ECD), which
197 best explains the measured data, was computed by
198 using a least-squares search. A subset of 16–18 chan-
199 nels including the local signal maxima was used for the
200 estimation of ECDs. These calculations gave the 3D
201 location, orientation, and strength of the ECD in a
202 spherical conductor model, which was based on each
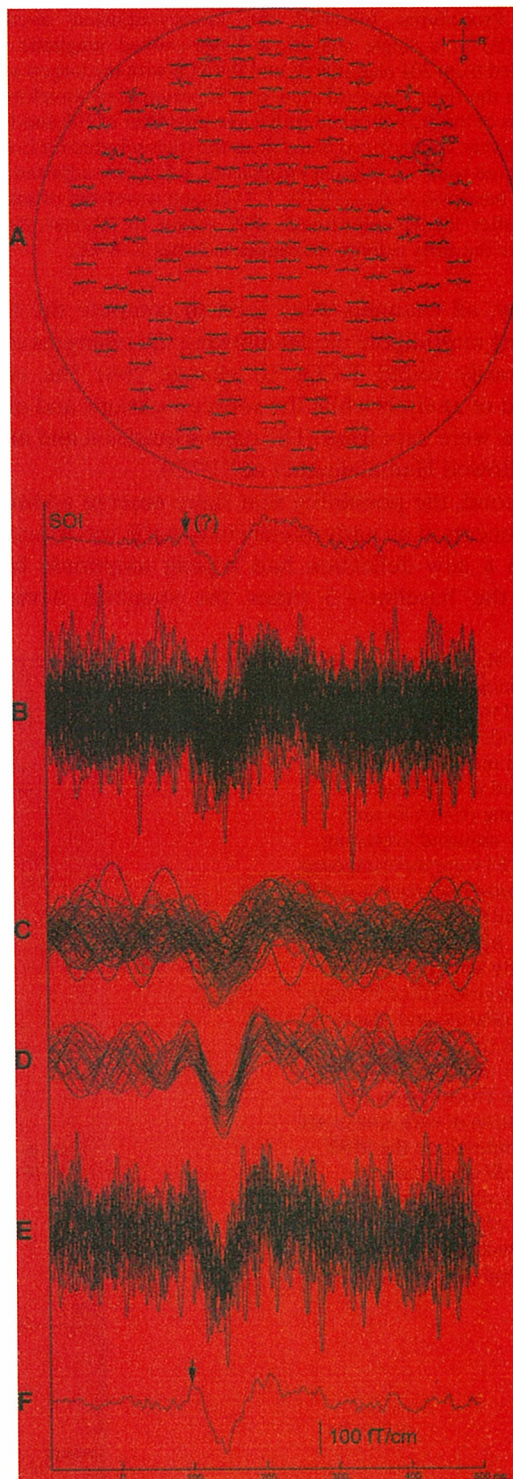
subject's MR images to show the source location. The 203
goodness-of-fit (GOF) value of an ECD was calculated 204
to indicate in percentage terms how much the dipole 205
accounts for the measured field variance. Only ECDs 206
explaining more than 85% of the field variance at 207
selected periods of time were used for further analysis. 208

◄Fig. 1 Procedures followed for latency-adjusted averaging (L-AVE) in a single subject. **a** Laser-evoked magnetic fields recorded from 204 planar coils and the SOI with the largest amplitude in the right temporal area. **b, c** Superimposed waveforms of 60 trials of the SOI obtained with a low-pass filter of 100 and 15 Hz, respectively. **c** *Waveforms in red* show the trials selected for L-AVE. **d** Selected trials were latency-corrected. **e** Latency-adjusted trials with a bandpass of 0.1–100 Hz. **f** Averaged waveform of selected trials after latency-adjustment. *SOI* sensor of interest. *Arrows* indicate the early activity that appeared after L-AVE

209 Finally, all channels were used to compute the time-
210 varying multidipole model allowing the strengths of the
211 previously found ECDs to change over the entire
212 period of analysis while the source locations and orien-
213 tations were kept fixed. The data acquisition and analy-
214 sis followed Hamalainen et al. (1993).
215   Second, the possibility that there emerge additional
216 components at an early latency in L-AVE was examined.
217 When a new deflection had a peak amplitude larger
218 than the baseline + 3 times the standard deviation

219 (SD), we accepted it as a significant component. In the
220 present study, the onset latency of a component was
221 defined as a latency point where the amplitude first
222 exceeded the baseline + 2 SD.
223   Data were expressed as the mean ± SD. A paired t-test
224 was used to compare the source's location and peak
225 amplitude between the C-AVE and L-AVE. A one-way
226 analysis of variance (ANOVA) was used to compare
227 the latency among cortical sources. P values less than
228 0.05 were considered to be significant.

Results 229

230 After the application of our criteria, 27–35 (mean 30.7)
231 trials were included for L-AVE in each subject, which
232 corresponded to 45–58% of the 60 trials used for C-AVE.
233   Figure 2a shows evoked magnetic fields recorded
234 from 204 planar gradiometers in C-AVE (black lines)

Fig. 2 Magnetic fields following noxious laser stimulation applied to the dorsum of the left hand. **a** Waveforms of evoked magnetic fields obtained in conventional averaging (C-AVE) and latency-adjusted averaging (L-AVE) were superimposed. The *upper right figures* show enlarged waveforms recorded from **a**, **b**, and **c**. *Arrows* show the early activities. **b, d** The time-varying source strength of cSI, cParaS, and iParaS in C-AVE (*lower left*) and L-AVE (*lower right*), respectively. **c** The location and orientation of each source are superimposed on the MRI scans. *cSI* contralateral primary somatosensory cortex, *cParaS* contralateral parasylvian region, *iParaS* ipsilateral parasylvian region
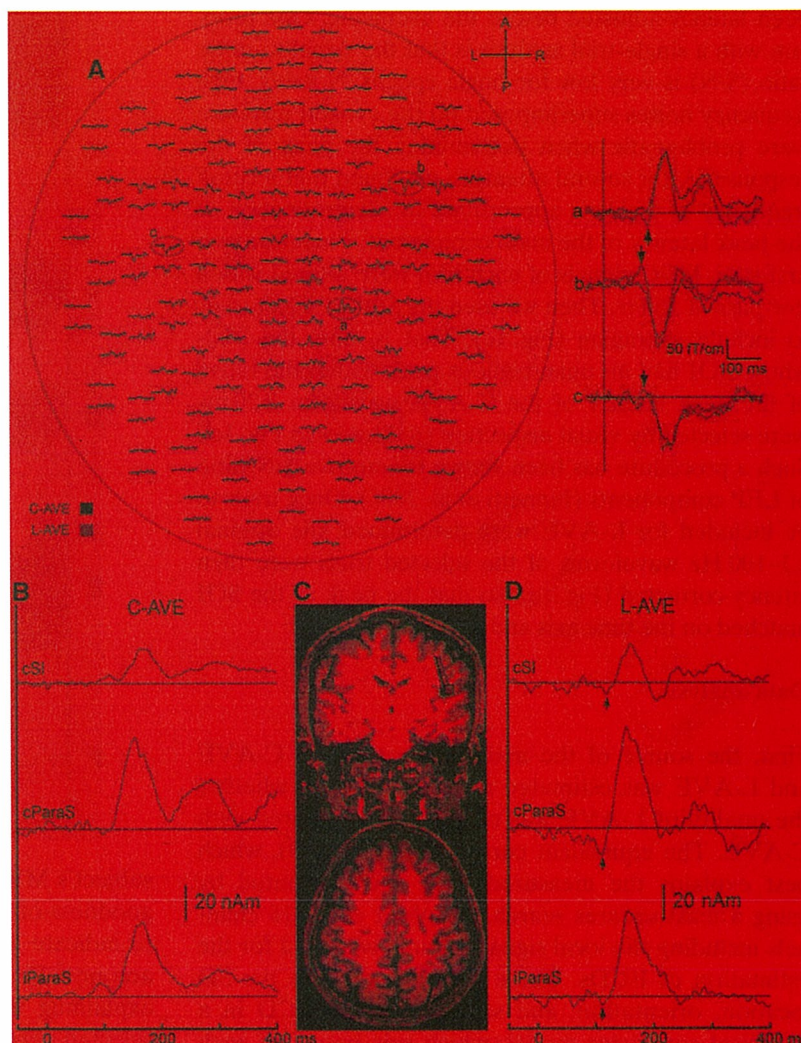
235 and L-AVE (red lines). Both in C-AVE and L-AVE,
236 a clear and consistent main component, which has
237 been reported in previous studies, was recorded in
238 three cortical areas; the left (contralateral) parietal
239 region and bilateral temporal regions. An ECD analy-
240 sis and subsequent superposition of sources on indi-
241 vidual MR images revealed that ECDs responsible
242 for these three main components were located around
243 the postcentral gyrus of the contralateral hemisphere
244 and around the upper bank of the Sylvian fissure or
245 near the insular circular sulcus of both hemispheres,
246 corresponding to the contralateral SI (cSI), contralateral
247 parasylvian region (cParaS), and ipsilateral parasyl-
248 vian region (iParaS), respectively. This three-source
249 model is compatible with previous laser-evoked
250 MEG studies (Ploner et al. 1999; Kanda et al. 2000;
251 Timmermann et al. 2001; Nakata et al. 2004). The
252 location of each cortical activity is shown in Table 1.
253 The location of each source in L-AVE did not differ
254 significantly from that in C-AVE (Fig. 2c). The GOF
255 for the cSI (94.7 ± 3.7) and cParaS (97.1 ± 2.7) sources

256 was significantly larger in L-AVE than in C-AVE
257 (91.1 ± 5.0 and 94.9 ± 4.6, respectively). The GOF
258 for the iParaS showed no significant difference
259 between C-AVE (95.8 ± 2.9) and L-AVE (94.6 ±
260 1.6) ($P = 0.25$). The onset and peak latency of the
261 main deflection in the three cortical areas did not
262 differ significantly between C-AVE and L-AVE
263 (Table 2). In both C-AVE and L-AVE, the onset or
264 peak latency for iParaS was significantly longer than
265 that for cSI or cParaS. The onset latency did not
266 differ between cSI and cParaS (Table 2). The time-
267 varying source strength in each region is shown in
268 Fig. 2b, d. The peak amplitude of the three main
269 activities was significantly greater in L-AVE than in
270 C-AVE (Table 3). ECD locations of these three
271 regions showed no significant difference between C-AVE
272 and L-AVE, indicating that the new method, L-AVE,
273 was reliable.
274 In addition to the main activities, early deflec-
275 tions were identified in the contralateral parietal
276 region and both temporal regions in both C-AVE
277 and L-AVE (Fig. 2a). However, early deflections in
278 C-AVE were very weak and usually did not meet
279 our criteria for a significant deflection. By contrast,
280 such deflections were identified more clearly in L-AVE.
281 In C-AVE, significant early deflections were identi-
282 fied in four subjects for cSI, four subjects for cParaS,
283 and three subjects for iParaS. After the L-AVE, sig-
284 nificant early deflections were identified in seven
285 subjects for cSI, in seven subjects for cParaS, and in
286 five subjects for iParaS. Usually significant deflec-
287 tions at early latencies were detected in three dis-
288 tinct areas; the contralateral parietal region and
289 both temporal regions, which were almost identical to
290 the locations for the three main components in C-AVE
291 (Fig. 3).
292 Figure 4 shows L-AVE waveforms of three channels
293 respectively selected from the contralateral parietal
294 region and bilateral temporal regions, in which the

Table 1 The mean location of each source for C-AVE and L-AVE

	x (mm)	y (mm)	z (mm)
C-AVE			
cSI	27.8 ± 9.7	11.9 ± 18.3	107.4 ± 11.7
cParaS	52.2 ± 7.5	33.4 ± 6.5	64.0 ± 10.2
iParaS	−53.3 ± 4.4	21.3 ± 4.1	71.3 ± 8.1
L-AVE			
cSI	27.6 ± 12.3	14.0 ± 17.5	107.7 ± 11.3
cParaS	54.0 ± 9.7	31.6 ± 8.1	63.6 ± 7.0
iParaS	−53.0 ± 4.7	21.2 ± 5.0	72.1 ± 7.7
Early-cSI ($n = 3$)	30.0 ± 11.4	10.8 ± 19.3	110.7 ± 6.6
Early-cParaS ($n = 5$)	52.9 ± 9.4	24.1 ± 13.7	62.9 ± 5.4
Early-iParaS ($n = 4$)	−53.3 ± 5.3	13.6 ± 11.8	67.8 ± 10.2

The x-axis passed through the preauricular points, the positive direction pointing to the right. The positive y-axis traversed the nasion. The positive z-axis pointed up. The location of each source did not differ between C-AVE and L-AVE

Table 2 The onset and peak latency of early and main deflections in L-AVE and C-AVE (ms)

	L-AVE				C-AVE			
	Early deflection		Main deflection		Early deflection		Main deflection	
	Onset	Peak	Onset	Peak	Onset	Peak	Onset	Peak
cSI	104.7 ± 16.8	118.7 ± 19.0	136.7 ± 13.5*	169.3 ± 16.4	104.0 ± 16.1	114.3 ± 15.4	134.6 ± 16.1*	168.1 ± 17.8
cParaS	88.1 ± 20.4	109.0 ± 12.9	136.0 ± 11.8*	163.0 ± 11.8*	84.3 ± 13.0	98.3 ± 4.9	131.1 ± 11.2*	163.9 ± 14.3*
iParaS	94.0 ± 17.1	111.8 ± 11.6	152.1 ± 14.4	180.7 ± 13.3	89.0 ± 23.5	115.0 ± 11.1	153.0 ± 14.5	181.3 ± 13.3

The number of subjects who showed a significant early deflection was seven, seven, and five in L-AVE, and four, four and three in C-AVE for cSI, cParaS, and iParaS, respectively

cSI contralateral primary somatosensory cortex, *cParaS* and *iParaS* contralateral and ipsilateral parasylvian regions, respectively

* $P < 0.05$, compared with iParaS (Fisher's PLSD procedure)

Table 3 The peak amplitude of early and main deflections in L-AVE and C-AVE (nAm)

	L-AVE		C-AVE	
	Early deflection	Main deflection	Early deflection	Main deflection
cSI	−35.3 ± 9.8	93.7 ± 31.7*	−29.6 ± 3.2	70.4 ± 23.1
cParaS	51.6 ± 21.8	−139.8 ± 33.9*	38.2 ± 17.6	−89.5 ± 19.8
iParaS	43.4 ± 18.1	−107.2 ± 17.2*	40.9 ± 8.5	−83.3 ± 15.3

The number of subjects who showed a significant early deflection was seven, seven, and five in L-AVE, and four, four, and three in C-AVE for cSI, cParaS, and iParaS, respectively

cSI contralateral primary somatosensory cortex, *cParaS* and *iParaS* contralateral and ipsilateral parasylvian regions, respectively

* $P < 0.01$, compared with the main deflection in C-AVE (paired t-test)

Fig. 3 Laser-evoked magnetic fields recorded from 204 planar coils in L-AVE in a single subject. The *waveform in grey* denotes that a significant early deflection prior to the main component is detected in this channel. *Arrows* and *asterisks* indicate the early and main deflection, respectively, with the largest amplitude in three areas around the contralateral parietal region and bilateral parasylvian regions. Significant early deflections are detected in the three cortical areas indicated by *circles*
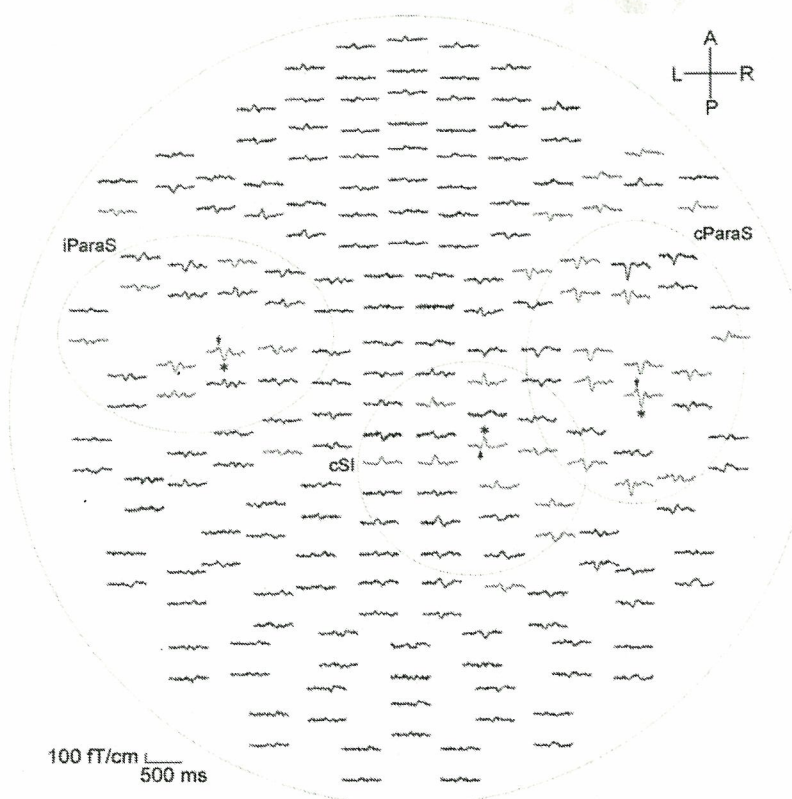
early and major deflections had the largest amplitude in all subjects (a) and ground-averaged waveforms (b). Figure 5 shows the waveform of the SOI and root mean square (RMS) of all subjects. For early deflections, a one-way ANOVA showed no significant difference in the onset and peak latencies among the three activities ($P = 0.48$), although the onset latency of cParaS tended to be shorter than that for cSI or iParaS (Table 2). The ECD of the early deflections could be estimated in three subjects for cSI, in five subjects for cParaS, and in four subjects for iParaS. In these samples, there was no consistent difference in the location of the source between the early and main activities (Table 1 and Fig. 6).

Discussion

In the present study, we found that three main activities originating from the contralateral SI and bilateral parasylvian regions and peaking at around 160–180 ms were responsible for laser-evoked magnetic fields. Both the locations and response latencies of the activities were consistent with previous MEG studies (Ploner et al. 1999; Kanda et al. 2000; Timmermann et al. 2001; Nakata et al. 2004), in which these activities have usually been considered the primary cortical response. However, in addition to these main activities, L-AVE in the present study revealed the presence of early activities in these three cortical areas peaking at
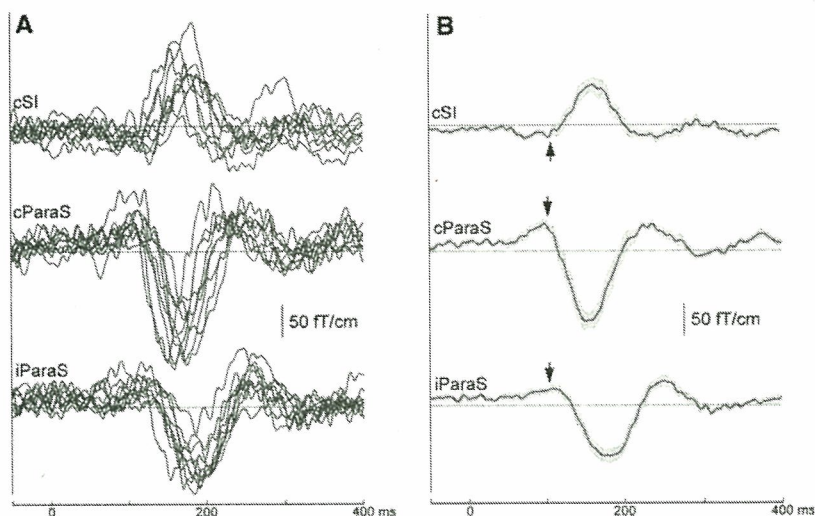
Fig. 4 a Superimposed wave-
forms of evoked magnetic
fields of all subjects recorded
form three channels, in which
the main components showed
the largest amplitude in the
contralateral parietal region
and bilateral temporal
regions, respectively.
b Group-averaged wave-
forms. *Shaded areas* depict
±SE. *Arrows* show the mean
peak latency of the early
responses

110–120 ms, indicating that the cortical processing of
information on pain took place earlier than previously
considered. Since the early component had an opposite
direction to that of the main component, the early
component is considered to be a discrete component
but is not a part of the main component. The onset
latencies (88–105 ms) of the early activities appear to
be appropriate for the earliest cortical activity given a
peripheral conduction velocity of 15 ms/s (Inui et al.
2002a, b) in A-delta fibers and 10–20 m/s in the spinal
cord (Kakigi and Shibasaki 1991; Cruccu et al. 2000;
Tsuji et al. 2006). Traveling at 15 m/s, it would take
roughly 80 ms to move from the hand to the cortex
(120 cm).

Methodological considerations

Before discussing the findings of L-AVE, we should
consider the possibility that the early activities
detected with L-AVE were artificial. We could exclude
this possibility based on the following. (1) In a few sub-
jects, there were significant early deflections prior to
the main deflections even in the C-AVE waveforms
though they were low in amplitude as compared to the
main deflections. (2) Although we used the peak
latency of the main component for the adjusting, the
L-AVE technique made both the early and main deflec-
tions clearer as compared to C-AVE. (3) Although we
selected the sensors with the largest amplitude around
the temporal area as SOIs and used them for adjusting
the latency of each trial, the quality of the data from SI
as well as the cParaS region was improved. Since the
early activity was low in amplitude and had the oppo-
site orientation to that of the main activity, we consid-
ered that it was easily cancelled out by the main
activity in the C-AVE process.

Cortical activations in SI and the parasylvian regions

In C-AVE, main activities were found to originate
from SI and the parasylvian regions, confirming previ-
ous findings (Ploner et al. 1999; Kanda et al. 2000; Tim-
mermann et al. 2001; Inui et al. 2002b; Nakata et al.
2004). The peak latency of the activity, 160–180 ms,
was consistent with results of previous MEG studies
using laser stimulation (Ploner et al. 1999; Kanda et al.
2000; Timmermann et al. 2001; Nakata et al. 2004). In
addition, the simultaneous activation of SI and cParaS
and significantly later activation of iParaS were consis-
tent with a recent MEG study (Ploner et al. 1999). The
involvement of these cortical areas in pain processing
has also been demonstrated in PET (Talbot et al. 1991;
Casey et al. 1994) and fMRI studies (Gelnar et al. 1999;
Apkarian et al. 2000).

However, only two papers have described the early
activity prior to the main activity in SI (Inui et al.
2003a, b). The early activity identified in the contralat-
eral SI area in the present study seems to correspond to
that described by Inui et al. (2003a), who showed that
the onset latency of the early SI activity (80 ms) follow-
ing a noxious epidermal electrical stimulation was
shorter by 29 ms than that for the main parasylvian
activity (109 ms). Therefore, the temporal relationship
between the early SI and the main parasylvian activi-
ties was very similar to the present results showing a
latency delay of 31 ms. For the latter, the slightly
longer onset latency (105 ms) of the early SI activity in
the present study might be due to the temperature con-
duction time for laser stimulation.

As for the early activity in the parasylvian region,
there are two studies that reported its presence. Valeri-
ani et al. (2000) reported an early positive component
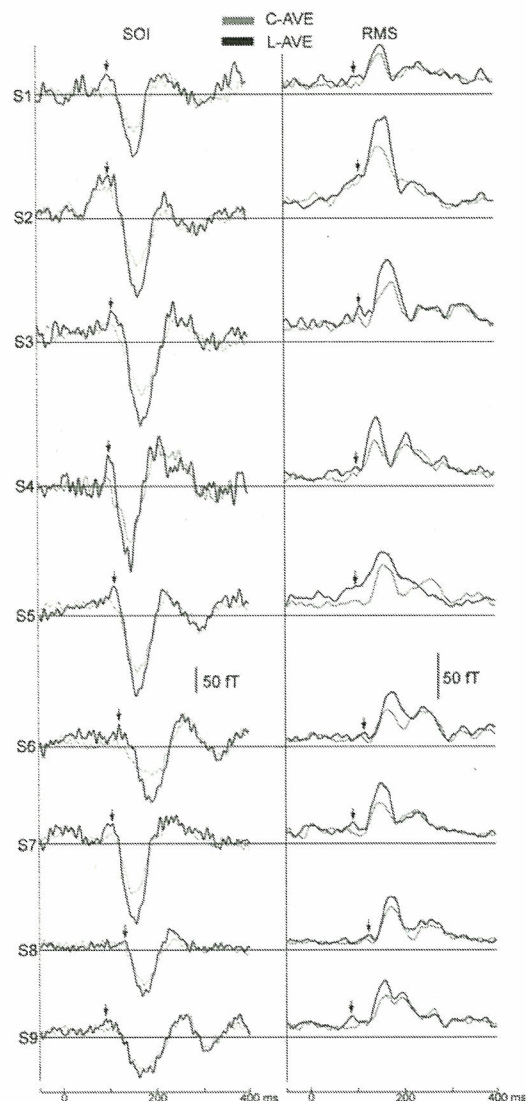(eP) in the contralateral parasylvian region with a peak

Fig. 5 The waveform of the SOI and RMS of nine subjects in C-AVE and L-AVE. *SOI* sensor of interest. *RMS* root mean square. *Arrows* indicate the early activity

391 latency of 83 ms that preceded the N1 negativity. Since
392 they used a CO_2 laser and we used a YAG laser to
393 elicit pain-related potentials, it is difficult to directly
394 compare the early component between their study and
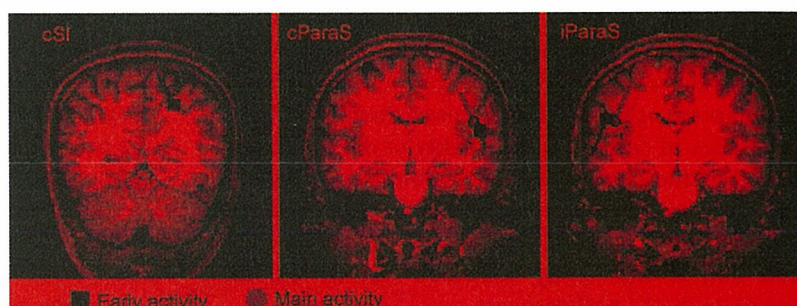
the present study. However, the early deflection in the 395
parasylvian region in the present study might corre- 396
spond to the eP of Valeriani et al. (2000). In both stud- 397
ies, the early component preceding the N1 component 398
had a small amplitude and an opposite orientation to 399
that of the N1 component. In another study using intra- 400
cranial recordings, Frot et al. (1999) demonstrated an 401
early negative response at a latency of 135 ms in the 402
parasylvian region, followed by a positive response 403
peaking around 170 ms, which seems to correspond to 404
the present early and main polarity-reversed activities. 405

As for the latency difference of the parasylvian 406
activity between hemispheres, the 17-ms delay for the 407
ipsilateral response of the main component in the pres- 408
ent study was consistent with results of the intracranial 409
recording study by Frot et al. (1999). In the study by 410
Frot et al. (1999) a similar time lag was also found for 411
the early component (15 ms). In the present study how- 412
ever, the latency of the early component did not differ 413
significantly among the three cortical areas. This dis- 414
crepancy was probably due to the low S/N ratio of the 415
early component or the small sample of data in the 416
present study. 417

The precise anatomical location of the early parasyl- 418
vian activity was not clear like the main activity in this 419
region. The location of nociceptive cortical areas 420
around the sylvian fissure is still a matter of contro- 421
versy. It has been difficult to determine whether the 422
nociceptive area is situated within the classic SII (pari- 423
etal operculum) or within an adjacent somatosensory 424
area such as the frontoparietal operculum or insula. 425
Many previous studies have shown that noxious stimuli 426
activate at least one cortical area around the sylvian 427
region other than SII. For example, fMRI (Bingel et al. 428
2003; Brooks et al. 2005; Iannetti et al. 2005) and intra- 429
cranial EEG (Lenz et al. 2000; Frot and Mauguiere 430
2003) studies found activation in the posterior insula 431
following noxious stimulation. Our previous studies 432
also showed that activity from the insula may contrib- 433
ute to the major MEG signals evoked by noxious stim- 434
uli (Inui et al. 2003a; Wang et al. 2004). In the present 435
study, the dipole was estimated to be located in the 436

Fig. 6 Source locations of early and main activities in a representative subject. The locations were almost the same, but the dipole's direction was opposite

437 upper bank of the sylvian fissure in some cases but
438 deeper around the circular sulcus in others. Therefore,
439 we consider that activation in the sylvian region in this
440 study may be a summation of activities from SII and
441 adjacent areas. With regard to the early parasylvian
442 activity, a reliable estimation of its source could not be
443 obtained in some subjects because of the low S/N ratio.
444 However, the sources of the early deflections were esti-
445 mated to lie around the bilateral parasylvian region in
446 the other subjects with a GOF of more than 85%.
447 These findings suggested that the early components
448 originated from similar regions to the main activities.

449 Temporal sequence of activation

450 The present results showing the simultaneous onset of
451 the main SI and contralateral parasylvian activities are
452 consistent with recent MEG studies (Ploner et al.
453 1999). These findings support the notion of a parallel
454 mode of pain processing between the SI and parasyl-
455 vian region. However, the temporal sequence of corti-
456 cal activation should be reconsidered because of the
457 presence of earlier activities. Our results suggested that
458 early cortical processing of noxious information occurs
459 earlier than previous neurophysiological studies have
460 estimated. As for the early component, our results did
461 not find a significant difference in latency among the
462 three cortical areas. However, this could be due to the
463 small number of subjects, or due to the low S/N ratio of
464 these activities. The slightly shorter latency of the con-
465 tralateral parasylvian source compared to the other
466 two sources might suggest the dominance of the con-
467 tralateral parasylvian region in the early processing of
468 noxious information.

469 **References**

470 Apkarian AV, Gelnar PA, Krauss BR, Szeverenyi NM (2000)
471 Cortical responses to thermal pain depend on stimulus size:
472 a functional MRI study. J Neurophysiol 83:3113–3122
473 Apkarian AV, Bushnell MC, Treede RD, Zubieta JK (2005)
474 Human brain mechanisms of pain perception and regulation
475 in health and disease. Eur J Pain 9:463–484
476 Bingel U, Quante M, Knab R, Bromm B, Weiller C, Buchel C
477 (2003) Single trial fMRI reveals significant contralateral bias
478 in responses to laser pain within thalamus and somatosen-
479 sory cortices. Neuroimage 18:740–748
480 Bromm B, Treede RD (1984) Nerve fibre discharges, cerebral
481 potentials and sensations induced by CO$_2$ laser stimulation.
482 Hum Neurobiol 3:33–40
483 Brooks JC, Zambreanu L, Godinez A, Craig AD, Tracey I (2005)
484 Somatotopic organisation of the human insula to painful
485 heat studied with high resolution functional imaging. Neuro-
486 image 27:201–209
487 Casey KL, Minoshima S, Berger KL, Koeppe RA, Morrow TJ,
488 Frey KA (1994) Positron emission tomographic analysis of
489 cerebral structures activated specifically by repetitive nox-
490 ious heat stimuli. J Neurophysiol 71:802–807
491 Craig AD, Bushnell MC, Zhang ET, Blomqvist A (1994) A tha-
492 lamic nucleus specific for pain and temperature sensation.
493 Nature 372:770–773
494 Cruccu G, Iannetti GD, Agostino R, Romaniello A, Truini A,
495 Manfredi M (2000) Conduction velocity of the human spino-
496 thalamic tract as assessed by laser evoked potentials. Neuro-
497 report 11:3029–3032
498 Frot M, Mauguiere F (2003) Dual representation of pain in the
499 operculo-insular cortex in humans. Brain 126:438–450
500 Frot M, Rambaud L, Guenot M, Mauguiere F (1999) Intracortical
501 recordings of early pain-related CO$_2$-laser evoked potentials
502 in the human second somatosensory (SII) area. Clin Neuro-
503 physiol 110:133–145
504 Gelnar PA, Krauss BR, Sheehe PR, Szeverenyi NM, Apkarian
505 AV (1999) A comparative fMRI study of cortical represen-
506 tations for thermal painful, vibrotactile, and motor perfor-
507 mance tasks. Neuroimage 10:460–482
508 Gingold SI, Greenspan JD, Apkarian AV (1991) Anatomic evi-
509 dence of nociceptive inputs to primary somatosensory cor-
510 tex: relationship between spinothalamic terminals and
511 thalamocortical cells in squirrel monkeys. J Comp Neurol
512 308:467–490
513 Hamalainen M, Hari R, Ilmoniemi RJ, Knuutila J, Lounasmaa
514 OV (1993) Magnetoencephalography—theory, instrumenta-
515 tion, and applications to non-invasive studies of the working
516 human brain. Rev Mod Phys 65:413–497
517 Hari R, Portin K, Kettenmann B, Jousmaki V, Kobal G (1997)
518 Right-hemisphere preponderance of responses to painful CO$_2$
519 stimulation of the human nasal mucosa. Pain 72:145–151
520 Huttunen J, Kobal G, Kaukoranta E, Hari R (1986) Cortical
521 responses to painful CO$_2$ stimulation of nasal mucosa; a
522 magnetoencephalographic study in man. Electroencepha-
523 logr Clin Neurophysiol 64:347–349
524 Iannetti GD, Zambreanu L, Cruccu G, Tracey I (2005) Opercu-
525 loinsular cortex encodes pain intensity at the earliest stages
526 of cortical processing as indicated by amplitude of laser-
527 evoked potentials in humans. Neuroscience 131:199–208
528 Inui K, Tran TD, Hoshiyama M, Kakigi R (2002a) Preferential
529 stimulation of A delta fibers by intra-epidermal needle elec-
530 trode in humans. Pain 96:247–252
531 Inui K, Tran TD, Qiu Y, Wang X, Hoshiyama M, Kakigi R
532 (2002b) Pain-related magnetic fields evoked by intra-epider-
533 mal electrical stimulation in humans. Clin Neurophysiol
534 113:298–304
535 Inui K, Tran TD, Qiu Y, Wang X, Hoshiyama M, Kakigi R
536 (2003a) A comparative magnetoencephalographic study of
537 cortical activations evoked by noxious and innocuous
538 somatosensory stimulations. Neuroscience 120:235–248
539 Inui K, Wang X, Qiu Y, Nguyen BT, Ojima S, Tamura Y, Nakata
540 H, Wasaka T, Tran TD, Kakigi R (2003b) Pain processing
541 within the primary somatosensory cortex in humans. Eur J
542 Neurosci 18:2859–2866
543 Kakigi R, Shibasaki H (1991) Estimation of conduction velocity
544 of the spino-thalamic tract in man. Electroencephalogr Clin
545 Neurophysiol 80:39–45
546 Kakigi R, Koyama S, Hoshiyama M, Kitamura Y, Shimojo M,
547 Watanabe S (1995) Pain-related magnetic fields following
548 painful CO$_2$ laser stimulation in man. Neurosci Lett 192:45–48
549 Kakigi R, Watanabe S, Yamasaki H (2000) Pain-related somato-
550 sensory evoked potentials. J Clin Neurophysiol 17:295–308
551 Kakigi R, Inui K, Tran DT, Qiu Y, Wang X, Watanabe S, Hoshiyama
552 M (2004) Human brain processing and central mechanisms of
553 pain as observed by electro- and magneto-encephalography.
554 J Chin Med Assoc 67:377–386

555 Kanda M, Nagamine T, Ikeda A, Ohara S, Kunieda T, Fujiwara
556 N, Yazawa S, Sawamoto N, Matsumoto R, Taki W, Shibasaki
557 H (2000) Primary somatosensory cortex is actively involved
558 in pain processing in human. Brain Res 853:282–289
559 Kenshalo DR Jr, Giesler GJ Jr, Leonard RB, Willis WD (1980)
560 Responses of neurons in primate ventral posterior lateral
561 nucleus to noxious stimuli. J Neurophysiol 43:1594–1614
562 Kenshalo DR Jr, Chudler EH, Anton F, Dubner R (1988) SI noci-
563 ceptive neurons participate in the encoding process by which
564 monkeys perceive the intensity of noxious thermal stimula-
565 tion. Brain Res 454:378–382
566 Lamour Y, Willer JC, Guilbaud G (1983) Rat somatosensory
567 (SmI) cortex: I. Characteristics of neuronal responses to noxious
568 stimulation and comparison with responses to non-noxious
569 stimulation. Exp Brain Res 49:35–45
570 Lenz FA, Krauss G, Treede RD, Lee JL, Boatman D, Crone N,
571 Minahan R, Port J, Rios M (2000) Different generators in
572 human temporal-parasylvian cortex account for subdural
573 laser-evoked potentials, auditory-evoked potentials, and
574 event-related potentials. Neurosci Lett 279:153–156
575 Nakata H, Inui K, Wasaka T, Tamura Y, Tran TD, Qiu Y, Wang
576 X, Nguyen TB, Kakigi R (2004) Movements modulate
577 cortical activities evoked by noxious stimulation. Pain
578 107:91–98
579 Ohara S, Crone NE, Weiss N, Treede RD, Lenz FA (2004) Cuta-
580 neous painful laser stimuli evoke responses recorded directly
581 from primary somatosensory cortex in awake humans. J
582 Neurophysiol 91:2734–2746
583 Ploner M, Schmitz F, Freund HJ, Schnitzler A (1999) Parallel
584 activation of primary and secondary somatosensory cortices
585 in human pain processing. J Neurophysiol 81:3100–3104

586 Qiu Y, Noguchi Y, Honda M, Nakata H, Tamura Y, Tanaka S,
587 Sadato N, Wang X, Inui K, Kakigi R (2006) Brain processing
588 of the signals ascending through unmyelinated C fibers in
589 humans: an event-related functional magnetic resonance
590 imaging study. Cereb Cortex 16:1289–1295
591 Raij TT, Vartiainen NV, Jousmaki V, Hari R (2003) Effects of in-
592 terstimulus interval on cortical responses to painful laser
593 stimulation. J Clin Neurophysiol 20:73–79
594 Schlereth T, Baumgartner U, Magerl W, Stoeter P, Treede RD
595 (2003) Left-hemisphere dominance in early nociceptive pro-
596 cessing in the human parasylvian cortex. Neuroimage
597 20:441–454
598 Talbot JD, Marrett S, Evans AC, Meyer E, Bushnell MC, Duncan
599 GH (1991) Multiple representations of pain in human cere-
600 bral cortex. Science 251:1355–1358
601 Tarkka IM, Treede RD (1993) Equivalent electrical source anal-
602 ysis of pain-related somatosensory evoked potentials elicited
603 by a CO_2 laser. J Clin Neurophysiol 10:513–519
604 Timmermann L, Ploner M, Haucke K, Schmitz F, Baltissen R,
605 Schnitzler A (2001) Differential coding of pain intensity in
606 the human primary and secondary somatosensory cortex. J
607 Neurophysiol 86:1499–1503
608 Tsuji T, Inui K, Kojima S, Kakigi R (2006) Multiple pathways
609 for noxious information in the human spinal cord. Pain
610 123:322–331
611 Valeriani M, Restuccia D, Le Pera D, Fiaschetti L, Tonali P,
612 Arendt-Nielsen L (2000) Unmasking of an early laser
613 evoked potential by a point localization task. Clin Neuro-
614 physiol 111:1927–1933
615 Wang X, Inui K, Qiu Y, Kakigi R (2004) Cortical responses to
616 noxious stimuli during sleep. Neuroscience 128:177–186

PAIN

Multiple pathways for noxious information in the human spinal cord

Takeshi Tsuji [a,b,*], Koji Inui [a], Seiji Kojima [b], Ryusuke Kakigi [a,c]

[a] *Department of Integrative Physiology, National Institute for Physiological Sciences, Myodaiji, Okazaki 444-8585, Japan*
[b] *Department of Pediatrics, Nagoya University Graduate School of Medicine, Nagoya 466-8550, Japan*
[c] *RISTEX, Japan Science and Technology Agency, Japan*

Abstract

To investigate the pathways of noxious information in the spinal cord in humans, we recorded cortical potentials following the stimulation of A-delta fibers using a YAG laser applied to two cutaneous points on the back at the C7 and Th10 level, 4 cm to the right of the vertebral spinous process. A multiple source analysis showed that four sources were activated; the primary somatosensory cortex (SI), bilateral parasylvian region (Parasylvian), and cingulate cortex. The activity of the cingulate cortex had two components (N2/P2). The mean peak latencies of the activities obtained by C7 and Th10 stimulation were 166.9 and 186.0 ms (SI), 144.3 and 176.8 ms (contralateral Parasylvian), 152.7 and 185.5 ms (ipsilateral Parasylvian), 186.2 and 215.8 ms (N2), and 303.0 and 332.3 ms (P2). Estimated spinal conduction velocities (CVs) of the respective activities were 16.8, 9.3, 8.7, 10.1 and 10.7 m/s. CV of SI was significantly faster than the others ($P < 0.05$). Therefore, our results suggested that noxious signals were conveyed through at least two distinct pathways of the spinal cord probably reaching distinct groups of thalamic nuclei. Further studies are required to clarify the functional significance of these two pathways.
© 2006 International Association for the Study of Pain. Published by Elsevier B.V. All rights reserved.

Keywords: Pain; Spinothalamic tracts; Conduction velocity; Electroencephalography; Laser evoked potential

1. Introduction

Noxious stimuli applied to the skin surface are detected by nociceptors in the epidermis (Burgess and Perl, 1967; Beitel and Dubner, 1976). The signals are conveyed through thinly myelinated A-delta-fibers and unmyelinated C-fibers to reach the dorsal horn of the spinal cord (Light and Perl, 1979; Sugiura et al., 1986). In the spinal cord, two different groups of neurons receive inputs from the periphery, that is, neurons in the superficial lamina (mainly lamina I) and deep lamina (mainly lamina V). Therefore, the processing of noxious signals in separate systems starts at the spinal level (Craig, 2003; Price et al., 2003). Nociceptive-specific

(NS) neurons in lamina I respond to cold and noxious stimuli (Christensen and Perl, 1970; Kumazawa et al., 1975; Dostrovsky and Craig, 1996), while wide dynamic range (WDR) neurons in lamina V respond to both noxious and innocuous stimuli (Wall, 1960; Mendell, 1966; Willis et al., 1974). Then they project to distinct thalamic regions, although their terminations partly overlap (Apkarian and Hodge, 1989a). Spinothalamic neurons in lamina I mainly project to the medial thalamic nuclei and possibly to posterior part of the ventral medial nucleus (VMpo), while those in lamina V mainly project to the ventral posterior lateral nucleus (VPL) (Kenshalo et al., 1980; Ralston and Ralston, 1992; Craig et al., 1994). Furthermore, these thalamic nuclei have distinct projection sites. That is, VPL, VMpo, and medial thalamic nuclei mainly project to the primary somatosensory cortex (SI), the insula, and the anterior cingulate cortex (ACC), respectively (for review, see Treede

* Corresponding author. Tel.: +81 564 55 7814; fax: +81 564 52 7913.
E-mail address: ttsuji@nips.ac.jp (T. Tsuji).

et al., 1999). Considering the different response properties of neurons and different anatomical pathways, these two streams of nociceptive processing appear to differ in function. In spite of these findings in animal studies, the functional and anatomical segregation in humans is still a subject of controversy, since less is known about segregated nociceptive processing largely due to the limitations of experimental methods. Notably, whether there are distinct pathways in the spinal cord itself is not well understood.

Therefore in the present study, we sought to clarify multiple spinal pathways for nociceptive processing in humans. We recorded cerebral evoked potentials (EPs) following Tm:YAG laser stimulation applied to two different levels of the right side of the back to measure the conduction velocity (CV) of signals in the spinothalamic tracts (STT). Previous studies in animals showed that pathways from the dorsal horn neurons in lamina I and lamina V to the thalamus had different CVs (Ferrington et al., 1987). Therefore, we considered that different pathways would have distinct CVs also in humans.

2. Methods

The experiment was performed on 10 healthy right-handed male volunteers, aged 22–36 years (mean, 29.3 ± 4.0). The study was approved in advance by the Ethics Committee of the National Institute for Physiological Sciences and written consent was obtained from all the subjects.

2.1. Noxious stimulation

For noxious stimulation, we used a Tm:YAG laser (Neurolaser, Baasel Lasertech, Germany). The wavelength was 2000 nm, pulse duration was 1 ms, and spot diameter was 6 mm. Laser stimuli were applied to two sites: the right side of the back 4 cm lateral to the 7th cervical vertebral spinous process (C7) and 10th thoracic vertebral spinous process (Th10). We chose these sites for stimulation to minimize the peripheral conduction distance of primary neurons, and stimulate the peripheral nerve of one side. In our previous report (Inui et al., 2006), we confirmed that the back is one of the cutaneous areas at which noxious stimulation evokes clear brain responses. Also, Cruccu et al. (2000) and Iannetti et al. (2003) obtained good results after noxious stimulation of the back. Histologically, the intraepidermal nerve fiber density of the trunk is higher than that of the distal leg (Lauria et al., 1999). The threshold for a pinprick sensation in the trunk is lower than that in the extremities (Agostino et al., 2000). The stimuli were delivered randomly at an interval of 10–15 s. The irradiated points were moved slightly within a transverse 4 cm area centered on the points after each stimulus to avoid tissue damage and habituation of the receptors. Subjects were asked to rate the intensity of the perceived pricking pain on a visual analogue scale (VAS, 0–10) prior to the experiment, and the stimulus intensity was adjusted to the level eliciting a VAS score of around seven.

2.2. EP recordings

Subjects lay prone on a bed and were asked to relax their muscles and keep their eyes open. The room temperature was 25 °C and sound and light were regulated. Skin temperature was kept above 30 °C (Kakigi and Shibasaki, 1991). A simultaneously recorded electro-oculogram (EOG) was used for artifact rejection. Signals were recorded with a band-pass filter of 0.1–100 Hz. The window of analysis was 600 ms including 100 ms of a prestimulus period, and the sampling rate was 1000 Hz. Laser stimuli were applied to C7 and Th10 randomly. For each site of stimulation, over 25 artifact-free trials were selected and averaged off-line. To minimize endogenous factors, subjects were asked not to predict which site would be stimulated and not to pay attention to the stimulated sites.

2.3. Source modeling

We recorded EPs using the standard 19 electrodes of the 10–20 system (Fp1, Fp2, F3, F4, F7, F8, Fz, C3, C4, Cz, T3, T4, T5, T6, P3, P4, Pz, O1, O2) and an additional 13 electrodes including FC1, FC2, C1, C2, C5, C6, T9, T10, CP1, CP2, P1, P2 and CPz (Fig. 1). The electrode impedance was always kept below 5 kΩ. We used the balanced non-cephalic reference (BNP, Stephenson and Gibbs, 1951), to reduce problems due to activities of the reference. We linked two electrodes, one from over the right sternoclavicular junction and the other from over the tip of the 7th cervical spine, and incorporated a variable resistor. By adjusting the resistance, the pickup of cardiac potentials was minimized.

Since several cortical activities following noxious stimulation overlapped temporally, we analyzed theoretical multiple source generators of EPs using the brain electric source analysis (BESA) software package (NeuroScan, Inc, Mclean, VA, USA). Model adequacy was assessed by examining: (i) percent variance; (ii) F-ratio (ratio of reduced χ^2 values before and after adding a new source); and (iii) residual waveforms
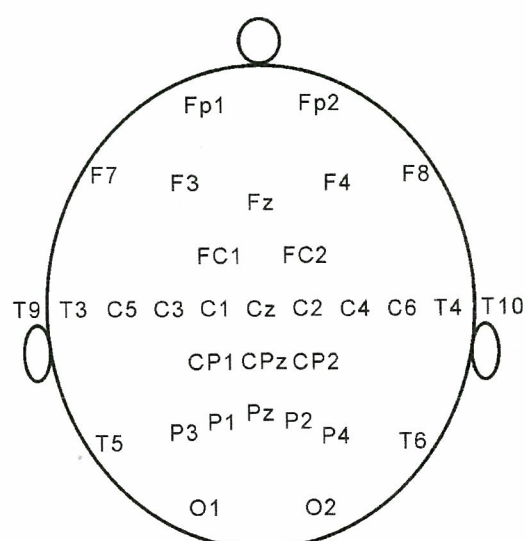

Fig. 1. Locations of the 32 electrodes.

(i.e., the difference between the recorded data and the model) as described elsewhere (Inui et al., 2004). Percent variance measures the goodness of fit (GOF) of the model comparing the recorded data and the model. The integral probability of obtaining a F-ratio value equal to or greater than the obtained value is calculated to evaluate whether a model with a larger number of dipoles represents a statistical improvement of the fit over a model with a smaller number of dipoles. When a P value was <0.05, we considered the new dipole as significant. BESA uses a spherical 4 shell model with an 85 mm radius. The spatial position of each dipole is defined by reference points on the head known as fiducials. The reference points are nasion, the left preauricular point (T9), and the right pre-auricular point (T10). The x axis is defined by the line joining T9 and T10, positive towards T10. The y axis is defined by the line through nasion that is perpendicular to the x axis (positive towards nasion). The z axis is perpendicular to the x and y axes, and goes up out of the head in the vicinity of Cz.

2.4. Measuring conduction velocities

The CV of a given nerve fiber can be calculated by mea-suring the difference in response latency of cerebral potentials between two different stimulation sites. For example, by dividing the distance between hand and arm stimulation sites by the latency difference of evoked potentials following hand and arm stimulations, one can estimate the CV of the periph-eral nerve. By use of laser-evoked potentials (LEPs), the CV of A-delta fibers can be measured (Kenton et al., 1980; Bromm and Treede, 1987). By use of similar methods, CVs in STT were also measured (Kakigi and Shibasaki, 1991; Cruccu et al., 2000; Rossi et al., 2000; Qiu et al., 2001; Ian-netti et al., 2003).

In the present study, the spinal conduction time was tak-en from the difference in the peak latency of each cortical activity between C7 and Th10 stimulation. Although the onset latency is desirable when examining the timing of the arrival of nociceptive signals in a cortical area, its deter-mination was difficult. Therefore, we used the peak latency as in previous reports (Kakigi and Shibasaki, 1991; Cruccu et al., 2000; Rossi et al., 2000; Qiu et al., 2001; Iannetti et al., 2003). The peak latency was the latency point with the maximal amplitude. The CV was calculated by dividing the distance between C7 and Th10 by the difference in laten-cy of each activity.

In the present study, we had an interest in the spinal con-duction time, not in other conduction times. So, even though the peak latency does not directly reflect the conduction time calculated with the CV, it did not matter. For example, although the latency of P2 is too late for the CV, it would not result from the spinal cause (Kakigi and Shibasaki, 1991; Rossi et al., 2000; Iannetti et al., 2003). The latency difference could reflect the spinal conduction time.

2.5. Analysis

Data were expressed as means ± SD. The statistical signif-icance of the peak latencies of each stimulated site and CVs was assessed with a one-way analysis of variance (ANOVA). When the P value was less than 0.05, a post hoc analysis with the Bonferroni and Dunn method was performed.

3. Results

Fig. 2 shows results for a representative subject. Laser stimuli applied to C7 produced an activity at around 127 ms in the parasylvian region of both hemispheres. The topography also indicated a negativity around the parietal region contralateral to the stimulated side at around 149 ms. At later latencies, a large negativity at around 175 ms followed by a larger positivity at around 320 ms was evident and corresponded to well-known N2/P2 components (Kakigi et al., 2000). These topo-graphic findings indicated that at least four distinct sources were active during the period of analysis. There-fore, we analyzed the data using BESA to differentiate each source activity.

Isocontour maps at 127 ms in Fig. 2B show that bilat-eral sources around the sylvian region were active. To explain the data at this latency point, two sources were estimated to be located in the bilateral parasylvian region (Fig. 2E, a). Fig. 2C, a shows the theoretical distribution of these sources. This two-dipole model could explain 74.2% of the recorded EPs at 127 ms. Then we subtracted the theoretical waveforms of these sources from the recorded EPs (Fig. 2A, b). To explain the subtracted waveform, the best source was estimated in the midcingu-late cortex (MCC) based on the recent cytoarchitectonic subdivision by Vogt (2005) (Fig. 2E, b), which appears to correspond to a region described as the anterior cingu-late cortex in many previous reports. At a latency range from 175 to 450 ms, the addition of the MCC source markedly improved the fit (for example, the GOF value at 320 ms increased from 0.8% to 91.5%). We considered that this activity was compatible with the well-known N2/P2. This three-dipole model could explain 87.2% of the recorded EPs, but weak dipolar fields around the parietal region remained to be explained (Fig. 2A, c and D, a). To explain the residual waveform, the best source was esti-mated to be located in a parietal region slightly posterior to the central sulcus around the midline (Fig. 2E, c), which probably corresponds to the medial part of the postcentral gyrus of the contralateral hemisphere. With the addition of this source (SI source), the residual wave-forms in Fig. 2A, c were almost abolished. This four-source model provided a GOF value of 90.7%.

Similar results were obtained in the remaining sub-jects. The mean coordinates of each dipole are shown in Table 1. The SI source was located around the mid-line, which was compatible with the trunk area of SI. These results were similar to the four-dipole model after stimulation of the hand reported by Tarkka and Treede (1993) and Schlereth et al. (2003). The MCC source as the major contributor to EPs following stimulation of the back was also consistent with the results reported by Iannetti et al. (2003). Accordingly, five distinct activ-ities, SI, bilateral parasylvian activities (Pc and Pi) and MCC (N2/P2), were used to measure CVs.
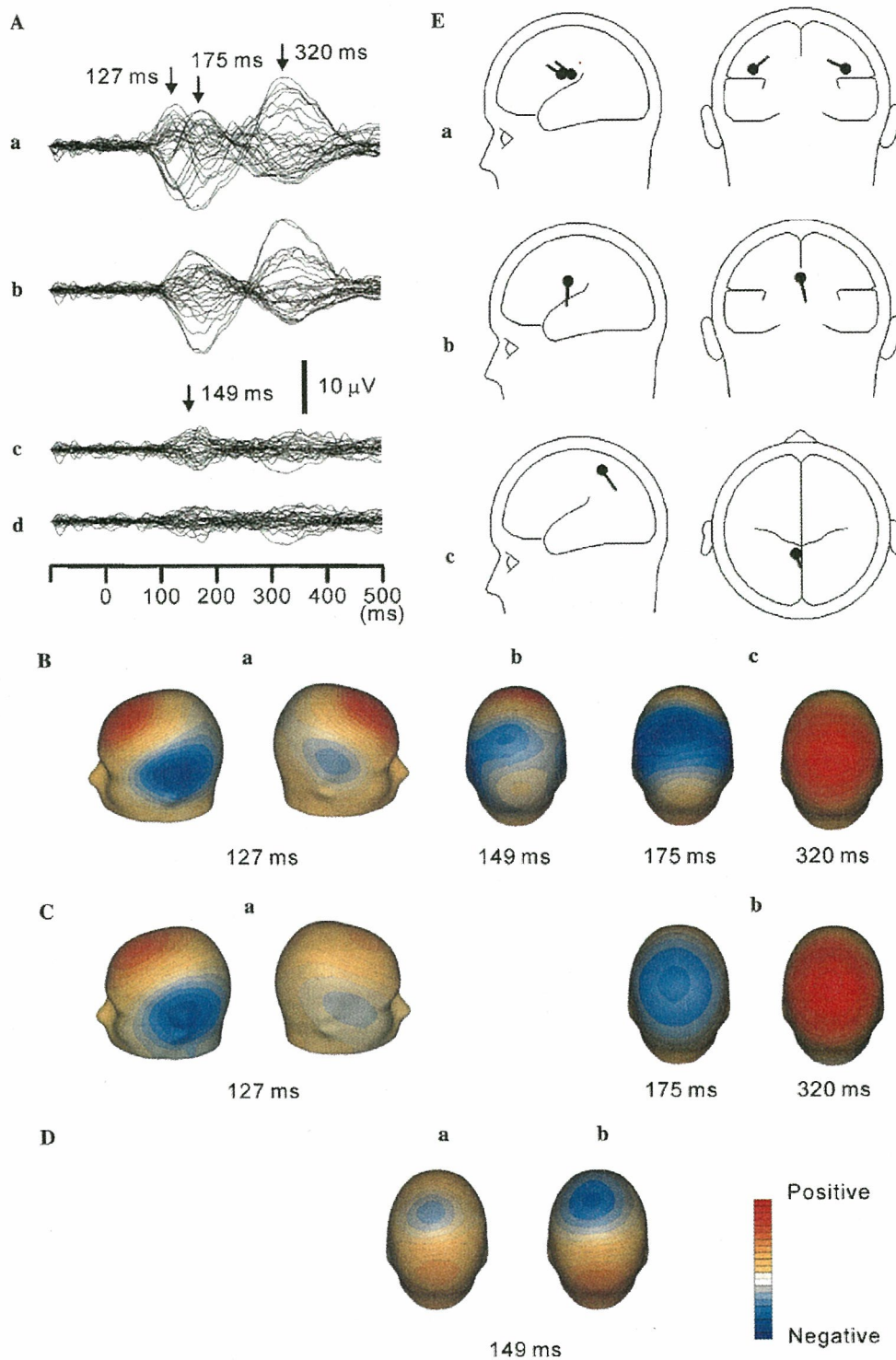
Fig. 2. Procedures of the multiple source analysis in a representative subject. First, two dipoles around the sylvian region (E, a) were estimated to explain the waveform recorded around 127 ms. B, a and C, a show isocontour maps of the recorded data and the two-dipole model at 127 ms, respectively. A, b shows the residual waveform obtained by the subtraction of the theoretical waveform due to these two sources from the recorded waveform (A, a). To explain the residual waveform (A, b), the best third source was estimated to be located in the cingulate cortex (E, b). B, c and C, b show isocontour maps of the recorded data and the third source model, respectively. A, c shows the residual waveform that remains to be explained by the three-dipole model. To explain the distribution of the residual waveform (D, a), the fourth source was estimated to lie around the medial part of the postcentral gyrus (E, c). D, b shows the theoretical field distribution of this source. After the fitting of these four sources, the residual waveform (A, d) showed no clear components.

Table 1
Locations of dipoles

	C7			Th10		
	x	y	z	x	y	z
SI	-4.8 ± 6.8	-16.6 ± 20.7	86.0 ± 8.4	-3.9 ± 6.5	-15.1 ± 19.1	87.4 ± 7.4
Pc	-45.3 ± 10.6	15.4 ± 4.8	56.3 ± 4.6	-45.1 ± 10.5	15.6 ± 7.2	55.6 ± 4.9
Pi	47.1 ± 12.2	15.0 ± 7.3	56.3 ± 5.7	47.6 ± 12.1	15.3 ± 7.2	56.0 ± 4.9
MCC	-3.1 ± 7.4	10.1 ± 12.9	56.8 ± 18.3	-0.6 ± 5.6	12.3 ± 15.8	59.5 ± 13.9

SI, primary somatosensory cortex; Pc, parasylvian source in the hemisphere contralateral to the stimulated side; Pi, parasylvian source in the hemisphere ipsilateral to the stimulated side; MCC, midcingulate cortex.

The peak latencies of each activity are shown in Table 2. An ANOVA showed that there was a significant difference in peak latency among the five activities following C7 stimulation ($F(1,4) = 218.8$, $P < 0.01$). The peak latency of P2 was significantly later than that of any other activities (post hoc test: $P < 0.01$), and the peak latency of N2 was also significantly later than that of SI, Pc or Pi (post hoc test: $P < 0.05$). On average, the peak latency of P2 was later than that of N2 by 116.8 ms, and in turn, the peak latency of N2 was later than that of SI, Pc and Pi by 19.3, 41.9 and 33.5 ms, respectively. The temporal relationship of each activity following Th10 stimulation was similar to that following C7 stimulation.

The estimated CVs of each activity are shown in Table 2. An ANOVA showed that there was a significant difference in CVs among the five activities ($F(1,4) = 6.4$, $P < 0.01$). The CV of SI was significantly greater than that of any other activities (post hoc test: $P < 0.05$). There was no significant difference among CVs for Pc, Pi, N2 and P2 (see Fig. 3).

4. Discussion

The present results clearly showed that at least two distinct pathways in the spinal cord transmitted noxious signals. This is the first report to confirm in the human spinal cord that nociceptive signals are processed by both the faster spinal CV pathway projecting to SI and the slower spinal CV pathway projecting to the parasylvian region and MCC.

4.1. Cortical activities

We identified activities in four cortical areas, SI, bilateral parasylvian regions and MCC, which is consistent with previous LEP studies (Tarkka and Treede, 1993; Schlereth et al., 2003). Previous LEP studies (Table 3) consistently found activities in the sylvian region. However, the locations of the parasylvian source were variable. Dipoles in electroencephalographic (EEG) and magnetoencephalographic (MEG) studies tend to be estimated in the upper bank of the sylvian fissure, while dipoles identified using subcortical and intracerebral recordings tended to be in deeper areas. MCC is an essential source in EEG studies, but not in MEG studies.

In previous studies, a somatotopic arrangement of SI activities after noxious stimulation to the hand and foot compatible with the well-known somatosensory homunculus has been reported in monkeys (Kenshalo et al., 2000) and humans (Penfield and Boldrey, 1937; Tarkka

Table 2
The peak latency of each source activity and estimated conduction velocity in the spinothalamic tract

Subject	Peak latency (ms)										Distance (cm)	Conduction velocity (m/s)				
	SI		Pc		Pi		N2		P2			SI	Pc	Pi	N2	P2
	C7	Th10	C7	Th10	C7	Th10	C7	Th10	C7	Th10						
1	157	178	146	181	153	192	187	221	285	321	28.5	13.6	8.1	7.3	8.4	7.9
2	184	207	128	149	157	184	175	194	324	350	27.5	12.0	13.1	10.2	14.5	10.6
3	180	198	144	169	152	180	171	204	327	345	26.5	14.7	10.6	9.5	8.0	14.7
4	148	173	134	170	153	183	194	216	331	354	27.2	10.9	7.6	9.1	12.4	11.8
5	161	171	150	170	155	183	194	219	283	302	26.8	26.8	13.4	9.6	10.7	14.1
6	178	190	159	184	159	187	185	214	315	336	26.0	21.7	10.4	9.3	9.0	12.4
7	171	202	139	199	149	180	188	239	293	338	27.5	8.9	4.6	8.9	5.4	6.1
8	174	187	149	186	146	199	186	205	287	322	28.5	21.9	7.7	5.4	15.0	8.1
9	144	172	140	179	136	174	165	191	278	330	27.5	9.8	7.1	7.2	10.6	5.3
10	172	182	154	181	167	193	217	255	307	325	27.8	27.8	10.3	10.7	7.3	15.4
Mean	166.9	186.0	144.3	176.8	152.7	185.5	186.2	215.8	303.0	332.3	27.4	16.8	9.3	8.7	10.1	10.7
SD	13.7	13.0	9.3	13.3	8.2	7.4	14.5	19.6	20.2	15.6	0.8	7.1	2.8	1.6	3.1	3.6

SI, primary somatosensory cortex; Pc, parasylvian source in the hemisphere contralateral to the stimulated side; Pi, parasylvian source in the hemisphere ipsilateral to the stimulated side.
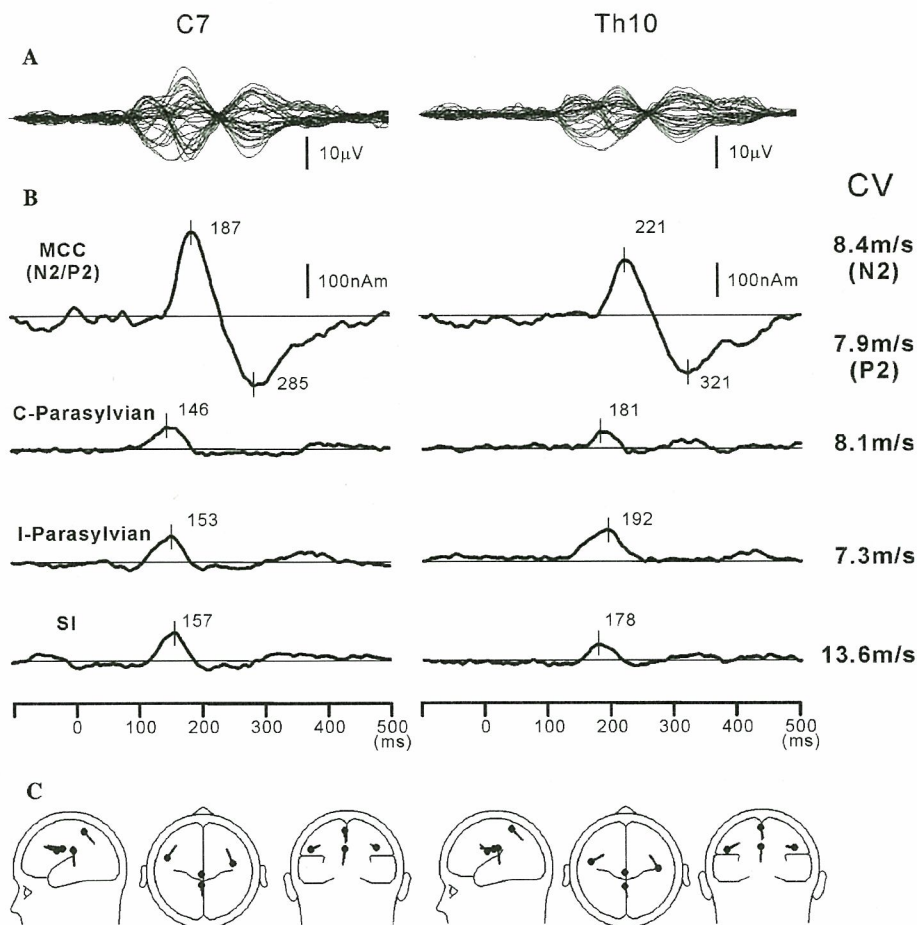
Fig. 3. Estimation of conduction velocity of each source activity in the spinal cord in a single subject. (A) Superimposed waveforms of evoked potentials following C7 (left) and Th10 (right) stimulation. (B) Time course of each cortical activity obtained by a multiple source analysis. (C) Schematic drawings of the location and orientation of each source. Estimated conduction velocity (CV) of each activity is shown. Note the similar latency difference between C7 and Th10 stimulation with the exception that the difference is smaller for the SI activity than the other source activities.

and Treede, 1993; Bingel et al., 2004; Ogino et al., 2005). These studies showed that the hand was represented in the lateral part of the postcentral gyrus and the foot, near the midline. These results imply that the pain system employs a body surface map in SI that is similar to the somatosensory homunculus. Since the representation of the trunk in SI in the somatosensory system is located around the midline, our results seem to support this idea. However, the precise location of nociceptive neurons in SI was slightly posterior to area 3b and probably in area 1, area 2 or the posterior parietal cortex in animals (Kenshalo and Isensee, 1983) and human studies (Kanda et al., 2000; Ploner et al., 2000; Inui et al., 2003; Ohara et al., 2004; Valeriani et al., 2004). The timing of SI activation in the present study was consistent with previous EEG and MEG studies (Tarkka and Treede, 1993; Ploner et al., 1999; Inui et al., 2003).

Our multiple source analysis showed that bilateral parasylvian EP components come from the sylvian region. Although previous LEP studies agreed that this

activity was generated in the secondary somatosensory cortex (SII) area (Tarkka and Treede, 1993; Bromm and Chen, 1995; Kakigi et al., 1995; Valeriani et al., 1996), recent subdural LEP studies showed that it was generated in the frontoparietal operculum overlying insula, not in the parietal operculum overlying SII (Lenz et al., 2000; Vogel et al., 2003). In functional magnetic resonance imaging (fMRI) studies, both SII and the insula were activated by noxious stimuli (Brooks et al., 2002; Bingel et al., 2003). Our previous MEG study using noxious intraepidermal electrical stimulation (Inui et al., 2003) showed that the insula was activated almost simultaneously with SII, although the results could not be directly compared with those of the present study because of different stimulus and recording conditions. The precise anatomical area responsible for this activity has not yet been determined. Therefore, we considered that parasylvian activity in the present study might be a summation of several temporally overlapping activities from the sylvian region.

Table 3
Source locations in previous studies (scalp EEG, MEG, subdural, and intracerebral)

Reference	Recording	Laser	Activated cortical area
Tarkka and Treede (1993)	EEG	CO_2	SI, SII, ACC
Bromm and Chen (1995)	EEG	CO_2	SII, ACC, frontal cortex
Kakigi et al. (1995)	MEG	CO_2	SII
Valeriani et al. (1996)	EEG	CO_2	SII, CC, mesial-temporal cortex
Watanabe et al. (1998)	MEG	CO_2	SII, amygdala-hippocampal formation
Lenz et al. (1998a)	Subdural	CO_2	Parietal operculum and/or insula
Lenz et al. (1998b)	Subdural	CO_2	ACC
Yamasaki et al. (1999)	MEG	CO_2	SII
Ploner et al. (1999)	MEG	YAG	SI, SII
Frot et al. (1999)	Intracerebral	CO_2	Frontoparietal operculum
Valeriani et al. (2000)	EEG	CO_2	SII, CC, insular-temporal cortex
Ploner et al. (2000)	MEG	YAG	SI (area 1), SII
Kanda et al. (2000)	MEG	CO_2	SI (area 1), SII
Lenz et al. (2000)	Subdural	CO_2	Parietal operculum–insula
Timmermann et al. (2001)	MEG	YAG	SI, SII
Frot et al. (2001)	Intracerebral	CO_2	Frontoparietal operculum
Ploner et al. (2002)	MEG	YAG	SI, SII, ACC
Iannetti et al. (2003)	EEG	CO_2	ACC
Schlereth et al. (2003)	EEG	YAG	SI, ACC, operculum
Vogel et al. (2003)	Subdural	CO_2	Frontoparietal operculum
Frot and Mauguiere (2003)	Intracerebral	CO_2	Operculum–insula
Valeriani et al. (2004)	Subdural	CO_2	SI (area 1, 2 or posterior parietal cortex)
Ohara et al. (2004)	Subdural	YAG	SI (not area 3b or 1), parasylvian area, ACC, SMA

SI, primary somatosensory cortex; SII, secondary somatosensory cortex; ACC, anterior cingulate cortex; SMA, supplementary motor area.

The main source generator was located in MCC, also in accordance with previous reports (Iannetti et al., 2003). Activation in these areas following noxious stimuli is consistent with fMRI studies (Bornhovd et al., 2002). Therefore, these five activities (SI, Pc, Pi, N2 and P2) were consistent with previous studies. We measured CVs of the STT using these five activities.

4.2. Methodological considerations when measuring CV

CVs of noxious signals in the human spinal cord were reported for the first time by Kakigi and Shibasaki (1991). They estimated CV by comparing the latencies of P2 following laser stimulation to the hand and foot. Although their method was confirmed later by Rossi et al. (2000), its peripheral component was not negligible. Recently, Cruccu et al. (2000) measured CV using EPs after stimulation of the dorsal midline. Since the back midline has the shortest conduction distance from the stimulated point to the spinal cord, this method has the advantage of reducing the peripheral components. In the present study, we stimulated two different levels of the right side of the back 4 cm lateral to the midline. This method had an additional advantage over previous studies in that it activated nociceptors belonging to the peripheral nerve of one side. Since noxious stimuli activate several cortical areas bilaterally with a 15–20 ms delay for the ipsilateral activity (Inui et al., 2003), the evoked response should be very complicated when stimuli are applied to the

midline. That is, responses in one hemisphere contain both contralateral and ipsilateral responses due to the stimulation of peripheral nerves of both sides. Another methodological advantage of this study was the random stimulation paradigm. The EP waveform is substantially affected by level of arousal, attention and expectancy (Kakigi et al., 2000). Our method could minimize such effects.

4.3. CV in the spinal cord

The estimated CVs in the spinal cord following noxious stimulation in the present study were 8.7–16.8 m/s. The CVs calculated from the peak latency of N2 (Cruccu et al., 2000), P2 (Kakigi and Shibasaki, 1991; Rossi et al., 2000) and N1/P1 (Rossi et al., 2000) were 21, 10 (8–12) and 10.0 m/s, respectively. Therefore, values in the present study were approximately consistent with those in other studies. The CV for the SI activity has not been reported previously.

4.4. Two pathways in the STT

The STT neurons are functionally separated into NS and WDR neurons. The locations are also different, namely, NS cells are mainly located in lamina I and WDR cells are mainly present in lamina V. Axons of NS and WDR cells ascend in different parts of the STT (Apkarian and Hodge, 1989b; Craig, 2003). Furthermore, NS and WDR cells have distinct projection

targets in the thalamus, although their terminations partly overlap (Apkarian and Hodge, 1989a; Willis and Westlund, 1997). As for the CV, signals of WDR cells conduct in the STT significantly faster than those of NS cells in monkeys (Ferrington et al., 1987). In this study, the CV for SI was significantly faster than that of any other activity, implying that activation in SI came from WDR cells. This notion is consistent with the fact that lamina V WDR neurons predominantly project to VPL and in turn, VPL predominantly projects to SI (Kenshalo et al., 1980), and that the majority of nociceptive neurons both in VPL (Kenshalo et al., 1980) and in SI (Kenshalo and Isensee, 1983) are of the WDR type. Based on comparisons of neurophysiological data between humans and monkeys (Mayer et al., 1975; Price and Mayer, 1975), it has been demonstrated that WDR cells are responsible for the sensory aspect of pain.

On the other hand, signals from lamina I NS neurons ascend through the STT with a slower CV to reach the insula (Friedman and Murray, 1986) or cingulate cortex (Vogt et al., 1979) via medial nuclei of the thalamus and possibly VMpo (Ralston and Ralston, 1992; Craig et al., 1994; Craig, 2004). Therefore, MCC with a slower CV in the spinal cord in this study appeared to come from lamina I NS neurons. This idea is supported by the finding in a unitary recording study in animals (Koyama et al., 1998) and humans (Hutchison et al., 1999) that the cingulate cortex contains neurons that respond to noxious stimuli exclusively.

As for the parasylvian activity, various areas around the sylvian fissure have been reported as responsible (Table 3). If parasylvian activities reflect SII activity, our finding that the parasylvian activity had a slower spinal CV than the SI activity is congruent with the findings that VPI receives input from neurons in both lamina I and lamina V (Apkarian and Shi, 1994), and that the nociceptive neurons in VPI (Apkarian and Shi, 1994) and SII (Dong et al., 1989) are of both WDR and NS types. If parasylvian activities reflect the insular activity, the present findings are consistent with the lamina I NS cells-VMpo-insula pathway proposed by Craig et al. (1994). In the thalamus, intralaminar nuclei also relay noxious information from STT neurons to the sensory cortex. For example, the centrolateral nucleus (CL) receives inputs from STT neurons and projects to SI (Gindold et al., 1991) and SII (Stevens et al., 1993). Since a large percentage of SII-projecting thalamocortical neurons do not receive direct inputs from the spinal cord (Stevens et al., 1993), polysynaptic pathways to the thalamus, such as spinoreticulothalamic projections to the intralaminar nuclei, are possible. The present results could not clarify which spinal pathway with a slow CV is responsible for the parasylvian activity.

References

Agostino R, Cruccu G, Iannetti G, Romaniello A, Truini A, Manfredi M. Topographical distribution of pinprick and warmth thresholds to CO2 laser stimulation on the human skin. Neurosci Lett 2000;285:115–8.

Apkarian AV, Hodge CJ. Primate spinothalamic pathways: III. Thalamic terminations of the dorsolateral and ventral spinothalamic pathways. J Comp Neurol 1989a;288:493–511.

Apkarian AV, Hodge CJ. Primate spinothalamic pathways: II. The cells of origin of the dorsolateral and ventral spinothalamic pathways. J Comp Neurol 1989b;288:474–92.

Apkarian AV, Shi T. Squirrel monkey lateral thalamus. I. Somatic nociresponsive neurons and their relation to spinothalamic terminals. J Neurosci 1994;14:6779–95.

Beitel RE, Dubner R. Response of unmyelinated (C) polymodal nociceptors to thermal stimuli applied to monkey's face. J Neurophysiol 1976;39:1160–75.

Bingel U, Lorenz J, Glauche V, Knab R, Glascher J, Weiller C, Buchel C. Somatotopic organization of human somatosensory cortices for pain: a single trial fMRI study. Neuroimage 2004;23:224–32.

Bingel U, Quante M, Knab R, Bromm B, Weiller C, Buchel C. Single trial fMRI reveals significant contralateral bias in responses to laser pain within thalamus and somatosensory cortices. Neuroimage 2003;18:740–8.

Bornhovd K, Quante M, Glauche V, Bromm B, Weiller C, Buchel C. Painful stimuli evoke different stimulus–response functions in the amygdala, prefrontal, insula and somatosensory cortex: a single-trial fMRI study. Brain 2002;125:1326–36.

Bromm B, Chen AC. Brain electrical source analysis of laser evoked potentials in response to painful trigeminal nerve stimulation. Electroencephalogr Clin Neurophysiol 1995;95:14–26.

Bromm B, Treede RD. Pain related cerebral potentials: late and ultralate components. Int J Neurosci 1987;33:15–23.

Brooks JC, Nurmikko TJ, Bimson WE, Singh KD, Roberts N. fMRI of thermal pain: effects of stimulus laterality and attention. Neuroimage 2002;15:293–301.

Burgess PR, Perl ER. Myelinated afferent fibers responding specifically to noxious stimulation of the skin. J Physiol 1967;190:541–62.

Christensen BN, Perl ER. Spinal neurons specifically excited by noxious or thermal stimuli: marginal zone of the dorsal horn. J Neurophysiol 1970;33:293–307.

Craig AD. Pain mechanisms: labeled lines versus convergence in central processing. Annu Rev Neurosci 2003;26:1–30.

Craig AD. Distribution of trigeminothalamic and spinothalamic lamina I terminations in the macaque monkey. J Comp Neurol 2004;477:119–48.

Craig AD, Bushnell MC, Zhang ET, Blomqvist A. A thalamic nucleus specific for pain and temperature sensation. Nature 1994;372:770–3.

Cruccu G, Iannetti GD, Agostino R, Romaniello A, Truini A, Manfredi M. Conduction velocity of the human spinothalamic tract as assessed by laser evoked potentials. Neuroreport 2000;11:3029–32.

Dong WK, Salonen LD, Kawakami Y, Shiwaku T, Kaukoranta EM, Martin RF. Nociceptive responses of trigeminal neurons in SII-7b cortex of awake monkeys. Brain Res 1989;484:314–24.

Dostrovsky JO, Craig AD. Cooling-specific spinothalamic neurons in the monkey. J Neurophysiol 1996;76:3656–65.

Ferrington DG, Sorkin LS, Willis WD. Responses of spinothalamic tract cells in the superficial dorsal horn of the primate lumbar spinal cord. J Physiol 1987;388:681–703.

Friedman DP, Murray EA. Thalamic connectivity of the second somatosensory area and neighboring somatosensory fields of the lateral sulcus of the macaque. J Comp Neurol 1986;252:348–73.

Frot M, Garcia-Larrea L, Guenot M, Mauguiere F. Responses of the supra-sylvian (SII) cortex in humans to painful and innocuous stimuli. A study using intra-cerebral recordings. Pain 2001;94:65–73.

Frot M, Mauguiere F. Dual representation of pain in the operculo-insular cortex in humans. Brain 2003;126:438–50.

Frot M, Rambaud L, Guenot M, Mauguiere F. Intracortical recordings of early pain-related CO2-laser evoked potentials in the human second somatosensory (SII) area. Clin Neurophysiol 1999;110:133–45.

Gindold SI, Ggreenspan JD, Apkarian AV. Anatomic evidence of nociceptive inputs to primary somatosensory cortex: relationship between spinothalamic terminals and thalamocortical cells in squirrel monkeys. J Comp Neurol 1991;308:467–90.

Hutchison WD, Davis KD, Lozano AM, Tasker RR, Dostrovsky JO. Pain-related neurons in the human cingulate cortex. Nat Neurosci 1999;2:403–5.

Iannetti GD, Truini A, Romaniello A, Galeotti F, Rizzo C, Manfredi M, et al. Evidence of a specific spinal pathway for the sense of warmth in humans. J Neurophysiol 2003;89:562–70.

Inui K, Tran TD, Qiu Y, Wang X, Hoshiyama M, Kakigi R. A comparative magnetoencephalographic study of cortical activations evoked by noxious and innocuous somatosensory stimulations. Neuroscience 2003;120:235–48.

Inui K, Tsuji T, Kakigi R. Temporal analysis of cortical mechanisms for pain relief by tactile stimuli in humans. Cereb Cortex 2006;16:355–65.

Inui K, Wang X, Tamura Y, Kaneoke Y, Kakigi R. Serial processing in the human somatosensory system. Cereb Cortex 2004;14:851–7.

Kakigi R, Koyama S, Hoshiyama M, Kitamura Y, Shimojo M, Watanabe S. Pain-related magnetic fields following painful CO2 laser stimulation in man. Neurosci Lett 1995;192:45–8.

Kakigi R, Shibasaki H. Estimation of conduction velocity of the spino-thalamic tract in man. Electroencephalogr Clin Neurophysiol 1991;80:39–45.

Kakigi R, Watanabe S, Yamasaki H. Pain-related somatosensory evoked potentials. J Clin Neurophysiol 2000;17:295–308.

Kanda M, Nagamine T, Ikeda A, Ohara S, Kunieda T, Fujiwara N, et al. Primary somatosensory cortex is actively involved in pain processing in human. Brain Res 2000;853:282–9.

Kenshalo DR, Giesler GJ, Leonard RB, Willis WD. Responses of neurons in primate ventral posterior lateral nucleus to noxious stimuli. J Neurophysiol 1980;43:1594–614.

Kenshalo DR, Isensee O. Responses of primate SI cortical neurons to noxious stimuli. J Neurophysiol 1983;50:1479–96.

Kenshalo DR, Iwata K, Sholas M, Thomas DA. Response properties and organization of nociceptive neurons in area 1 of monkey primary somatosensory cortex. J Neurophysiol 2000;84:719–29.

Kenton B, Coger R, Crue B, Pinsky J, Friedman Y, Carmon A. Peripheral fiber correlates to noxious thermal stimulation in humans. Neurosci Lett 1980;17:301–6.

Koyama T, Tanaka YZ, Mikami A. Nociceptive neurons in the macaque anterior cingulate activate during anticipation of pain. Neuroreport 1998;9:2663–7.

Kumazawa T, Perl ER, Burgess PR, Whitehorn D. Ascending projections from marginal zone (lamina I) neurons of the spinal dorsal horn. J Comp Neurol 1975;162:1–11.

Lauria G, Holland N, Hauer P, Cornblath DR, Griffin JW, McArthur JC. Epidermal innervation: changes with aging, topographic location, and in sensory neuropathy. J Neurol Sci 1999;164:172–8.

Lenz FA, Krauss G, Treede RD, Lee JL, Boatman D, Crone N, et al. Different generators in human temporal–parasylvian cortex account

for subdural laser-evoked potentials, auditory-evoked potentials, and event-related potentials. Neurosci Lett 2000;279:153–6.

Lenz FA, Rios M, Chau D, Krauss GL, Zirh TA, Lesser RP. Painful stimuli evoke potentials recorded from the parasylvian cortex in humans. J Neurophysiol 1998a;80:2077–88.

Lenz FA, Rios M, Zirh A, Chau D, Krauss G, Lesser RP. Painful stimuli evoke potentials recorded over the human anterior cingulate gyrus. J Neurophysiol 1998b;79:2231–4.

Light AR, Perl ER. Spinal termination of functionally identified primary afferent neurons with slowly conducting myelinated fibers. J Comp Neurol 1979;186:133–50.

Mayer DJ, Price DD, Becker DP. Neurophysiological characterization of the anterolateral spinal cord neurons contributing to pain perception in man. Pain 1975;1:51–8.

Mendell LM. Physiological properties of unmyelinated fiber projection to the spinal cord. Exp Neurol 1966;16:316–32.

Ogino Y, Nemoto H, Goto F. Somatotopy in human primary somatosensory cortex in pain system. Anesthesiology 2005;103:821–7.

Ohara S, Crone NE, Weiss N, Treede RD, Lenz FA. Cutaneous painful laser stimuli evoke responses recorded directly from primary somatosensory cortex in awake humans. J Neurophysiol 2004;91:2734–46.

Penfield W, Boldrey E. Somatic motor and sensory representation in the cerebral cortex of man as studied by electrical stimulation. Brain 1937;60:389–443.

Ploner M, Gross J, Timmermann L, Schnitzler A. Cortical representation of first and second pain sensation in humans. Proc Natl Acad Sci USA 2002;99:12444–8.

Ploner M, Schmitz F, Freund HJ, Schnitzler A. Parallel activation of primary and secondary somatosensory cortices in human pain processing. J Neurophysiol 1999;81:3100–4.

Ploner M, Schmitz F, Freund HJ, Schnitzler A. Differential organization of touch and pain in human primary somatosensory cortex. J Neurophysiol 2000;83:1770–6.

Price DD, Greenspan JD, Dubner R. Neurons involved in the exteroceptive function of pain. Pain 2003;106:215–9.

Price DD, Mayer DJ. Neurophysiological characterization of the anterolateral quadrant neurons subserving pain in M. mulatta. Pain 1975;1:59–72.

Qiu Y, Inui K, Wang X, Tran TD, Kakigi R. Conduction velocity of the spinothalamic tract in humans as assessed by CO2 laser stimulation of C-fibers. Neurosci Lett 2001;311:181–4.

Ralston HJ, Ralston DD. The primate dorsal spinothalamic tract: evidence for a specific termination in the posterior nuclei (Po/SG) of the thalamus. Pain 1992;48:107–18.

Rossi P, Serrao M, Amabile G, Parisi L, Pierelli F, Pozzessere G. A simple method for estimating conduction velocity of the spinothalamic tract in healthy humans. Clin Neurophysiol 2000;111:1907–15.

Schlereth T, Baumgartner U, Magerl W, Stoeter P, Treede RD. Left-hemisphere dominance in early nociceptive processing in the human parasylvian cortex. Neuroimage 2003;20:441–54.

Stephenson WA, Gibbs FA. A balanced non-cephalic reference electrode. Electroencephalogr Clin Neurophysiol 1951;3:237–40.

Stevens RT, London SM, Apkarian AV. Spinothalamocortical projections to the secondary somatosensory cortex (SII) in squirrel monkey. Brain Res 1993;631:241–6.

Sugiura Y, Lee CL, Perl ER. Central projections of identified, unmyelinated (C) afferent fibers innervating mammalian skin. Science 1986;234:358–61.

Tarkka IM, Treede RD. Equivalent electrical source analysis of pain-related somatosensory evoked potentials elicited by a CO2 laser. J Clin Neurophysiol 1993;10:513–9.

Timmermann L, Ploner M, Haucke K, Schmitz F, Baltissen R, Schnitzler A. Differential coding of pain intensity in the human primary and secondary somatosensory cortex. J Neurophysiol 2001;86:1499–503.

Treede RD, Kenshalo DR, Gracely RH, Jones AK. The cortical representation of pain. Pain 1999;79:105–11.

Valeriani M, Barba C, Le Pera D, Restuccia D, Colicchio G, Tonali P, et al. Different neuronal contribution to N20 somatosensory evoked potential and to CO2 laser evoked potentials: an intracerebral recording study. Clin Neurophysiol 2004;115:211–6.

Valeriani M, Rambaud L, Mauguiere F. Scalp topography and dipolar source modeling of potentials evoked by CO2 laser stimulation of the hand. Electroencephalogr Clin Neurophysiol 1996;100:343–53.

Valeriani M, Restuccia D, Barba C, Le Pera D, Tonali P, Mauguiere F. Sources of cortical responses to painful CO(2) laser skin stimulation of the hand and foot in the human brain. Clin Neurophysiol 2000;111:1103–12.

Vogel H, Port JD, Lenz FA, Solaiyappan M, Krauss G, Treede RD. Dipole source analysis of laser-evoked subdural potentials recorded from parasylvian cortex in humans. J Neurophysiol 2003;89:3051–60.

Vogt BA. Pain and emotion interactions in subregions of the cingulate gyrus. Nat Rev Neurosci 2005;6:533–44.

Vogt BA, Rosene DL, Pandya DN. Thalamic and cortical afferents differentiate anterior from posterior cingulate cortex in the monkey. Science 1979;204:205–7.

Wall PD. Cord cells responding to touch, damage, and temperature of skin. J Neurophysiol 1960;23:197–210.

Watanabe S, Kakigi R, Koyama S, Hoshiyama M, Kaneoke Y. Pain processing traced by magnetoencephalography in the human brain. Brain Topogr 1998;10:255–64.

Willis WD, Trevino DL, Coulter JD, Maunz RA. Responses of primate spinothalamic tract neurons to natural stimulation of hindlimb. J Neurophysiol 1974;37:358–72.

Willis WD, Westlund KN. Neuroanatomy of the pain system and of the pathways that modulate pain. J Clin Neurophysiol 1997;14:2–31.

Yamasaki H, Kakigi R, Watanabe S, Naka D. Effects of distraction on pain perception: magneto- and electro-encephalographic studies. Brain Res Cogn Brain Res 1999;8:73–6.

Temporal Analysis of Cortical Mechanisms for Pain Relief by Tactile Stimuli in Humans

Koji Inui, Takeshi Tsuji and Ryusuke Kakigi

Department of Integrative Physiology, National Institute for Physiological Sciences, Myodaiji, Okazaki 444-8585, Japan

The mechanisms by which vibrotactile stimuli relieve pain are not well understood, especially in humans. We recorded cortical magnetic responses to paired noxious (intra-epidermal electrical stimulation, IES) and innocuous (transcutaneous electrical stimulation, TS) stimuli applied to the back at a conditioning–test interval (CTI) of −500 to 500 ms. Results showed that IES-induced responses were remarkably attenuated when TS was applied 20–60 ms later and 0–500 ms earlier than IES (CTI = −60 to 500 ms). Since the signals evoked by IES reached the spinal cord (CTI = −60 to −20 ms conditions) and the cortex (−60 and −40 ms condition) earlier than those evoked by TS, the present results indicate that cortical responses to noxious stimuli can be inhibited by innocuous tactile stimuli at the cortical level, with minimal contribution at the spinal level.

Keywords: intra-epidermal electrical stimulation, magnetoencephalogram, pain relief, transcutaneous electrical stimulation, vibrotactile stimuli

Introduction

Pain relief by vibrotactile stimuli is a well-known phenomenon. Although vibrotactile stimuli actually reduce experimental pain in animals (Woolf et al., 1977) and humans (Wall and Cronly-Dillon, 1960), and pathological pain in patients (Wall and Sweet, 1967; Meyer and Fields, 1972), the underlying mechanisms of this inhibition are still largely unknown. Notably, whether such an inhibition of nociception occurs at the cortical level has not been investigated at all. Many previous studies have considered the dorsal horn of the spinal cord as an important site for this phenomenon where large myelinated fiber inputs are said to affect the central transmission of signals from nociceptors (Melzack and Wall, 1965). In the present study, we demonstrate that cortical responses to noxious stimuli can be substantially inhibited by innocuous tactile stimuli with minimal contribution at the periphery or spinal cord.

Materials and Methods

Nine healthy male volunteers aged 24–40 (mean 31.1) years participated in this study. The study was approved in advance by the Ethical Committee of the National Institute for Physiological Sciences and written consent was obtained from all the subjects. Experiments were conducted according to the Declaration of Helsinki.

Stimulation

For a test noxious stimulation, we used an intra-epidermal electrical stimulation (IES) method that we recently developed (Inui et al., 2002a) for the selective stimulation of cutaneous A-delta fibers. However, the original method was modified slightly to provide high selectivity for the activation of nociceptors at a stronger intensity of stimulation than that used in previous studies (Inui et al., 2002a,b, 2003a,b). We used a stainless steel concentric bipolar needle electrode (patent pending) for IES. The anode was an outer ring 1.2 mm in

diameter and the cathode was an inner needle that protruded 0.2 mm from the outer ring. By pressing the electrode against the skin gently, the needle tip was inserted in the epidermis and superficial part of the dermis where nociceptors are located, while the outer ring was attached to the skin surface. Two electrodes 5 mm apart were used for augmentation of the response. The two electrodes were placed in parallel with the midline of the back. The electrical stimulus was current constant double pulses at 100 Hz with a 0.5 ms duration, and was applied to the right side of the back 4 cm lateral to the ninth thoracic vertebral spinous process. We chose this point since (i) the area around the back's midline is suitable for minimizing the conduction distance from the point of stimulation to the spinal cord; (ii) we wanted to stimulate the peripheral nerve of one side; and (iii) a lower point than the Th9 level would mean a longer conduction distance to the spinal cord while a higher point caused magnetic noise related to thoracic movements, that is, the stimulation electrode attached to the back moved with respiration and produced magnetic noise. The current intensity was at a level producing a definite pain sensation of ~40-60 in the visual analogue scale (VAS, 0-100) in each subject, where 0 represented no painful sensation and 100 represented an imaginary intolerable pain sensation. The mean stimulus intensity was 0.3 ± 0.08 mA. IES did not cause flare reactions around the electrode, an indication of C-fiber activation, like in our previous study (Inui et al., 2002a).

For a conditioning tactile stimulation, similar cutaneous sites were stimulated using a bipolar felt tip electrode (NM-420S, NihonKoden, Tokyo), 0.9 mm in diameter with a distance of 23 mm between the anode and cathode (transcutaneous electrical stimulation, TS). The felt tip electrode was placed just lateral to the concentric electrodes, and the center of them was 1 cm apart. The stimulus was double pulses at 100 Hz with 0.5 ms duration and the stimulus intensity was three times that of the sensory threshold (1.4 ± 0.2 mA) in each subject. Clear tactile sensations were elicited without any painful sensations using these stimulus parameters.

There were 13 stimulus conditions: control TS (conditioning stimulus alone), control IES (test stimulus alone) and 11 paired stimulus (IES + TS) conditions. In the eleven IES + TS conditions, paired stimuli were delivered with conditioning-test intervals (CTIs) of -500, -300, -100, -60, -40, -20, 0, 50, 100, 300 and 500 ms. Since the distance between the stimulus point and the corresponding level of the spinal cord is ~10 cm, it takes 1.7 ms for signals evoked by TS to reach the spinal cord at a conduction velocity of 60 m/s (A-beta fiber), while it takes 6.7 ms for signals due to ES at 15 m/s (A-delta fiber) (Inui et al., 2002a,b). Therefore, in the IES + TS -500 to -20 ms conditions, signals caused by IES are expected to reach the spinal cord earlier than those due to TS. Signals conveyed through peripheral A-beta and A-delta fibers also ascend in the spinal cord at different conduction velocities: A-beta fiber signals at 50-60 m/s and A-delta fiber signals at 8-10 m/s (Kakigi and Shibasaki, 1991). Given that the respective velocity is 60 and 9 m/s and the length of the spinal cord between C1 and T9 is 30 cm, the conduction time through the spinal cord in this study is 5 ms for TS and 33.3 ms for IES. Given the conduction time in the periphery and spinal cord, the difference in response latency at the cortex for TS and IES is expected to be ~33 ms. This means that in the IES + TS -500 to -40 ms conditions, signals due to IES reach the cortex earlier than those due to TS.